



# Manganese(II) complexes of pyridyl-appended diazacyclo-alkanes: Effect of ligand backbone ring size on catalytic olefin oxidation

Natarajan Saravanan<sup>a</sup>, Mallayan Palaniandavar<sup>a,b,\*</sup>

<sup>a</sup> Centre for Bioinorganic Chemistry, School of Chemistry, Bharathidasan University, Tiruchirappalli 620024, India

<sup>b</sup> Central University of Tamilnadu, Thiruvavur 610001, India

## ARTICLE INFO

### Article history:

Received 14 August 2011

Received in revised form 1 January 2012

Accepted 5 January 2012

Available online 28 January 2012

### Keywords:

Manganese(II) complexes

Diazacycloalkane ligands

Epoxidation

Electrochemistry

Catalytic properties

Iodosylbenzene

## ABSTRACT

A series of Mn(II) complexes [Mn(L)Cl<sub>2</sub>] **1–5**, where L is a tetradentate 4N ligand such as *N,N*-bis(2-pyridylmethyl)-1,2-diaminoethane (L1A), 1,4-bis(2-pyridylmethyl)piperazine (L2), *N,N*-bis(2-pyridylmethyl)hexahydropyrimidine (L3), *N,N*-bis(2-pyridylmethyl)-1,4-diazepane (L4) and *N,N*-bis(2-pyridylmethyl)-1,5-diazocane (L5), has been isolated, characterized by using electronic and ESI-MS spectral techniques and screened for catalytic olefin oxidation with a representative set of olefins. Interestingly, when the ligand *N,N*-bis(2-pyridylmethyl)imidazolidine (L1) is treated with MnCl<sub>2</sub>·6H<sub>2</sub>O in methanol it undergoes imidazolidine ring hydrolysis to form the complex [Mn(L1A)Cl<sub>2</sub>] possessing a distorted octahedral coordination geometry around Mn(II). The complex [Mn(L3)(OTf)<sub>2</sub>(H<sub>2</sub>O)] contains Mn(II) with a distorted pentagonal bipyramidal coordination geometry while [Mn(L4)Cl<sub>2</sub>] contains Mn(II) with an octahedral coordination geometry. The complex [Mn(L5)Cl<sub>2</sub>] adopts a rare trigonal prismatic coordination geometry, presumably because of steric interactions imposed by the ligand backbone. The catalytic ability of the solvent coordinated complex species [Mn(L)(ACN)<sub>2</sub>]<sup>2+</sup> show significant activity towards olefin epoxidation using iodosylbenzene (PhIO) as oxygen source and addition of *N*-methylimidazole to the reaction mixture increases the epoxide yield. The epoxidation of *cis*-cyclooctene catalyzed by the complexes proceeds with high conversion (22–65%) and selectivity (100%). The epoxide yield and product selectivity increase upon increasing the Lewis acidity of the Mn(II) center, as modified by the variation in the diazacycloalkane ligand backbone.

© 2012 Elsevier B.V. All rights reserved.

## 1. Introduction

Oxidation reactions are among the most elementary steps of all organic transformations and popular routes to prepare epoxides, which are valuable building blocks in synthetic organic chemistry and materials science [1]. The wide use of oxiranes as intermediates for production of fine chemicals as well as pharmaceuticals stimulated the development of oxidation technologies using oxygen donors such as molecular oxygen, peroxides, peracids, PhIO and its derivatives, sodium hypochlorite, etc. The development of catalytic epoxidation agents that are rapid, selective, scalable and inexpensive with a wide substrate scope remains an important goal. Since metalloenzymes catalyze the oxygenation reactions with high regio- and stereoselectivity under mild conditions, biomimetic oxygenation reactions using enzyme model compounds have attracted much attention among the communities of bioinorganic and oxidation chemistry [2]. Also, it is interesting that biological systems like cytochrome P450 [3], non-heme iron [4]

and Mn enzymes [5] are involved in the oxidation of alkanes, alkenes and related substrates [6]. As manganese is believed to be catalytically active in a variety of metalloenzymes [7], its chemistry has received considerable attention and manganese-based catalysts have been widely used for the oxidation of olefins to epoxides [8]. Although numerous procedures have been developed [9], the need to understand the mechanism of manganese mediated oxygenation processes demands the synthesis and study of new and already known catalysts.

Initial attempts using porphyrin-based catalysts with H<sub>2</sub>O<sub>2</sub> as oxidant for alkene epoxidation were unsuccessful due to dismutation of H<sub>2</sub>O<sub>2</sub> into H<sub>2</sub>O and O<sub>2</sub>, leading to fast depletion of the oxidant [10]. Many manganese porphyrins, which are able to catalyze the epoxidation of olefins with high efficiency using NaOCl [11], PhIO and its derivatives [12] and *m*-chloroperbenzoic acid (*m*-CPBA) [13] as oxidants, have been reported. Only a few non-heme monomeric Mn(II) complexes are known to be efficient epoxidation catalysts with H<sub>2</sub>O<sub>2</sub> [14]. Jacobsen et al. [15] and Katsuki and co-workers [16] have independently studied Mn–salen type complexes combined with special attention to asymmetric catalysis by using PhIO as oxidant and obtained highly enantioselective (89–98% enantiomeric excess) epoxidation by Mn–salen complexes derived from 1,2-diaminocyclohexane. Stack and

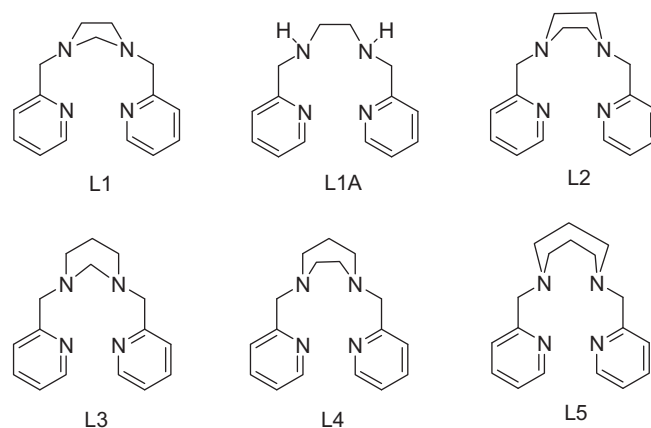
\* Corresponding author at: Central University of Tamilnadu, Thiruvavur 610001, India. Tel.: +91 431 2407125; fax: +91 431 2407043.

E-mail addresses: [palanim51@yahoo.com](mailto:palanim51@yahoo.com), [palaniandavarm@gmail.com](mailto:palaniandavarm@gmail.com) (M. Palaniandavar).

co-workers have screened a series of monomeric Mn(II) complexes of pyridine based ligands for olefin epoxidation reaction using peracetic acid and identified that  $[\text{Mn}(\text{bpy})_2(\text{OTf})_2]$  (bpy = 2,2'-bipyridine and OTf = trifluoromethanesulfonate) is the most active catalyst [17]. Costas et al. have described chiral Mn(II) complexes which are robust in epoxidising a wide range of olefins with good yields but show moderate selectivity (15–46% enantiomeric excess) under mild experimental conditions [18]. Very recently, Browne et al. showed that pyridine-2-carboxylic acid formed *in situ* via decomposition of TPTN/TPEN ligands combine with Mn salts to function as oxidation catalyst using  $\text{H}_2\text{O}_2$  in acetone as solvent [19]. It has been concluded that PhIO can be used as a single oxygen atom transfer reagent in a wide variety of studies with the purpose of generating reactive high-valent manganese-oxo intermediates analogous to those occurring in enzymatic reactions [20]. Also, Mn(II/III) complexes show highly selective epoxidation reactions using NaOCl and PhIO, which are considered to oxidize Mn(III)–salen complexes directly to the intermediate manganese-oxo species [21]. It is interesting to note that Nam and co-workers have also observed two different reactivities in alkane hydroxylation when PhIO and  $\text{CH}_3\text{COOOH}$  are used as oxidants [22].

In oxygen atom transfer processes catalyzed by Mn complexes of both heme and non-heme ligands, pentavalent  $\text{Mn}^{\text{V}}$  and  $\text{Mn}^{\text{V}}$  oxo moieties have been characterized by using various spectroscopic methods and X-ray crystallography and proposed as the active intermediate for alkane oxidation, olefin epoxidation, halogenations, electron-transfer reactions and photosynthetic water oxidation [23–30]. High-valent metal hydroxo complex species like peroxo manganic acid [29]  $[\text{Mn}^{\text{IV}}\text{L}(\text{O})(\text{OOH})]^+$  and  $[\text{Mn}^{\text{IV}}(\text{salen})(\text{OH})]$  with the sterically hindered salen platform [31] have been proposed as intermediates in catalytic oxidation reactions. Busch et al. have crystallographically characterized a mononuclear  $\text{Mn}^{\text{IV}}$  complex containing a pair of hydroxo ligands and an ultra rigid ethylene cross-bridged macrocyclic ligand. The mechanism of oxygen-atom transfer from such high-valent manganese-oxo intermediates to organic substrates has stimulated great interest as a result of its relevance to a wide range of important synthetic and biological pathway. Although significant progress has been made in this field, the effect of non-heme ligands on the oxidizing ability of the high-valent metal-oxo intermediate has been poorly understood. Also, the search for efficient, robust and recyclable catalysts remains an important task in homogeneous catalysis [32].

All the above observations prompted us to isolate Mn(II) complexes of a series of systematically varied tetradentate 4N ligands such as *N,N'*-bis(2-pyridylmethyl)-1,2-diaminoethane (bispicen, L1A), *N,N'*-bis(2-pyridylmethyl)piperazine (L2), *N,N'*-bis(2-pyridylmethyl)hexahydropyrimidine (L3), *N,N'*-bis(2-pyridylmethyl)-1,4-diazepane (L4) and *N,N'*-bis(2-pyridylmethyl)-1,5-diazocane (L5) (Scheme 1) and study the effect of diazacycloalkane backbone of tetradentate ligands on the catalytic activity of the complexes towards epoxidation of unfunctionalized olefins and also to understand the effect of the novel ligand systems in stabilizing manganese in higher oxidation states. The single crystal X-ray structures of the complexes  $[\text{Mn}(\text{L1A})\text{Cl}_2]$  **1**,  $[\text{Mn}(\text{L4})\text{Cl}_2]$  **4** and  $[\text{Mn}(\text{L5})\text{Cl}_2]$  **5** have been determined to show that the complexes contain two readily replaceable chloride ions in *cis* positions, which are convenient for catalytic olefin epoxidation. It would be interesting to obtain a correlation between the coordination geometry and reactivity of the complexes as the linear 4N ligands are expected to offer changes in coordination geometry around the metal center. The present Mn(II) complexes exhibit significant catalytic activity towards epoxidation of alkyl- and aryl-substituted olefins with high yields (54–84%) by using PhIO as the oxygen source. Also, the divergent flexibility as well as Lewis basicity of the ligands bound to Mn(II), as understood from the redox



Scheme 1. Ligands employed in this study.

potential of  $\text{Mn}^{\text{II}}/\text{Mn}^{\text{III}}$  couple, strongly influence the catalytic activity of the complexes.

## 2. Experimental

### 2.1. Materials

Pyridine-2-carboxaldehyde, ethane-1,2-diamine, propane-1,2-diamine, sodium triacetoxo-borohydride, sodium borohydride, piperazine, homopiperazine, 1,5-diazacyclooctane dihydrobromide, 2-picolychloride hydrochloride, iodobenzene diacetate, cyclooctene, cyclohexene, styrene (Aldrich), paraformaldehyde and triethylamine (Merck, India) were used as received. Acetonitrile, dichloromethane, ethylacetate, chloroform, diethylether, hexane (Merck, India) were used as received.

### 2.2. Synthesis of ligands

#### 2.2.1. General condensation procedure

A common two step procedure was followed for the syntheses of ligands L1 and L3 and the first step in the preparation of *N,N'*-bis(2-pyridylmethyl)-1,2-diaminoethane and *N,N'*-bis(2-pyridylmethyl)-1,2-diaminopropane, which were then reacted with paraformaldehyde in the second step to obtain L1 and L3, respectively.

**Step 1:** *N,N'*-Bis(2-pyridylmethyl)-1,2-diaminoethane (A) and *N,N'*-bis(2-pyridylmethyl)-1,2-diaminopropane (B) were prepared as reported [33] as yellow oils, respectively with 72% and 73% yields.  $^1\text{H NMR}$  (400 MHz,  $\text{CDCl}_3$ ): A:  $\delta$  2.25 (s, 3H), 2.65 (s, 2H), 3.15 (s, 2H), 7.4 (m, 3H), 8.45 (d, H); B: 1.70 (quint, H), 2.20 (s, 3H), 2.50 (s, 2H), 3.60 (s, 2H), 7.5 (m, 3H), 8.45 (d, H) ppm, respectively.

**Step 2:** *N,N'*-Bis(2-pyridylmethyl)imidazolidine (L1) and *N,N'*-bis(2-pyridylmethyl)-hexahydropyrimidine (L3) were prepared as reported [34] and isolated as dark yellow oils respectively with 76% and 79% yields.  $^1\text{H NMR}$  (400 MHz,  $\text{CDCl}_3$ ): L1:  $\delta$  (L1) 2.96 (s, 4H), 3.61 (s, 2H), 3.92 (s, 4H), 7.17 (t,  $J = 12.4$  Hz 2H), 7.48 (d,  $J = 7.6$  Hz 2H), 7.67 (t,  $J = 17.2$  Hz 2H), 8.55 (d,  $J = 5.6$  Hz 2H). L3:  $\delta$  (L3) 2.72 (s, 4H), 3.40 (s, 2H), 3.92 (s, 4H), 7.17 (t,  $J = 12.4$  Hz, 2H), 7.48 (d,  $J = 7.6$  Hz, 2H), 7.67 (t,  $J = 17.2$  Hz, 2H), 8.55 (d,  $J = 5.6$  Hz, 2H) ppm.

**2.2.1.1. Synthesis of *N,N'*-bis(2-pyridylmethyl)piperazine (L2).** This was prepared by using the procedure reported [35] already. Piperazine (1.010 g, 11.73 mmol) was treated with picolychloride hydrochloride (3.943 g, 24.04 mmol) to give L2 as a pale yellow crystalline solid, which was used for complex preparation without

further purification. Yield: 60%;  $^1\text{H}$  NMR ( $\text{CDCl}_3$ , 400 MHz)  $\delta$  2.57 (s, 8H), 3.67 (s, 4H), 7.15 (m, 2H), 7.39 (d, 2H), 7.64 (m, 2H), 8.55 (m, 2H) ppm.

**2.2.1.2. Synthesis of *N,N'*-bis(2-pyridylmethyl)-1,4-diazepane (L4).** This was prepared by reductive amination [36]. A mixture of homopiperazine (0.66 g, 6.22 mmol) and pyridine-2-carboxaldehyde (1.41 g, 13.2 mmol) was used to give L4 as a pale yellow oil, which is used for the complex preparation as such without further purification. Yield: 64%;  $^1\text{H}$  NMR ( $\text{CDCl}_3$ , 400 MHz) 1.74 (pentet,  $J = 5.9$  Hz, 2H), 2.67 (s, 4H), 2.71 (t,  $J = 5.8$  Hz, 4H), 3.72 (s, 4H), 7.03 (m, 2H), 7.37 (d, 2H), 7.54 (m, 2H),  $\delta$  8.43 (m, 2H) ppm.

**2.2.1.3. Synthesis of *N,N'*-bis(2-pyridylmethyl)-1,5-diazocane (L5).** The procedure used was similar to that used to prepare L2. A mixture of 1,5-diazacyclooctane dihydrobromide (2.327 g, 8.43 mmol) and picolylchloride hydrochloride (2.760 g, 16.83 mmol) was used to obtain L5 as a colorless crystalline solid, which was used for complex preparation without further purification. Yield: 68%;  $^1\text{H}$  NMR ( $\text{CDCl}_3$ , 400 MHz):  $\delta$  1.65 (pentet,  $J = 5.9$  Hz, 4H), 2.79 (t,  $J = 5.9$  Hz, 8H), 3.81 (s, 4H), 7.10 (m, 2H), 7.46 (m, 2H), 7.61 (m, 2H), 8.49 (m, 2H) ppm.

## 2.2.2. Synthesis of Mn(II) complexes

**2.2.2.1.  $[\text{Mn}(\text{L1A})\text{Cl}_2]$  (1).** To a solution of L1 (0.25 g, 1 mmol) in methanol (10 mL) was added  $\text{MnCl}_2 \cdot 4\text{H}_2\text{O}$  (0.20 g, 1 mmol) in methanol (5 mL), the solution stirred well and then cooled. The resultant brown solution was filtered and the filtrate was left to stand at room temperature for a week and a colorless precipitate was obtained. This was filtered off and washed with a few drops of ethanol, recrystallized from methanol and colorless crystals suitable for X-ray crystallography were grown by slow vapor diffusion of diethyl ether into a methanolic solution of the complex. Yield: 80%; *Anal. Calc.* for  $\text{C}_{14}\text{H}_{18}\text{Cl}_2\text{MnN}_4$ : C, 45.67; H, 4.93; N, 15.22. Found: C, 45.43; H, 4.62; N, 15.06%.

**2.2.2.2.  $[\text{Mn}(\text{L2})\text{Cl}_2]$  (2).** This complex was prepared by adding  $\text{MnCl}_2 \cdot 4\text{H}_2\text{O}$  (0.20 g, 1 mmol) in methanol (10 mL) to a solution of L2 (0.26 g, 1 mmol) in methanol, the solution stirred for 30 min, and then cooled. The off-white product was filtered off, washed with cold methanol and diethylether, and then dried under vacuum. Yield: 72%; *Anal. Calc.* for  $\text{C}_{16}\text{H}_{20}\text{Cl}_2\text{MnN}_4$ : C, 48.75; H, 5.11; N, 14.21. Found: C, 48.37; H, 5.10; N, 14.02%. ESI-MS of methanolic solution of **2** shows prominent peak at  $m/z$  values 347.6 and 382.13 corresponding to the  $[\text{Mn}_2(\text{L2})_2(\text{O})(\text{CH}_3\text{OH})]^{2+}$  and  $[\text{Mn}(\text{L2})\text{Cl} + \text{Na}]^+$ , respectively.

**2.2.2.3.  $[\text{Mn}(\text{L3})(\text{OTf})_2(\text{H}_2\text{O})]$  (3A).** The complex  $[\text{Mn}(\text{L3})\text{Cl}_2]$  **3** was prepared by adding  $\text{MnCl}_2 \cdot 4\text{H}_2\text{O}$  (0.20 g, 1 mmol) in methanol (5 mL) to a solution of L3 (0.26 g, 1 mmol) in methanol (10 mL), stirred for 30 min, and then cooled. The resulting solution was evaporated under vacuum and the residue was dissolved in  $\text{CH}_2\text{Cl}_2$ . ESI-MS of methanolic solution of **3** shows prominent peak at  $m/z$  values 411.5 and 457.20 corresponding to  $[\text{Mn}(\text{L3})(\text{H}_2\text{O})(\text{CH}_3\text{OH})\text{Cl}]^+$  and  $[\text{Mn}(\text{L3})(\text{H}_2\text{O})(\text{CH}_3\text{OH})_2\text{Cl}]^+$ , respectively. A solution of  $\text{AgOTf}$  (0.52 g, 2 mmol) in DCM (30 mL) was added and the mixture stirred in dark for 2 h under a nitrogen atmosphere. The solution was filtered, the volume reduced to approximately 5 mL under vacuum, and pentane was added to precipitate the product. This solid was subsequently washed with pentane and diethyl ether to give the product as a yellow orange powder. Yield: 63%. Crystals suitable for X-ray diffraction were grown from a  $\text{CH}_2\text{Cl}_2$ –pentane solution. *Anal. Calc.* for  $\text{C}_{18}\text{H}_{22}\text{F}_6\text{MnN}_4\text{O}_7\text{S}_2$ : C, 33.81; H, 3.47; N, 8.76. Found: C, 33.44; H, 3.21; N, 8.32%.

**2.2.2.4.  $[\text{Mn}(\text{L4})\text{Cl}_2]$  (4).** This complex was prepared in a manner analogous to that described for **2** using L4 instead of L2. Pale white crystals suitable for X-ray diffraction were grown from a slow evaporation methanolic solution of the complex. Yield: 76%; *Anal. Calc.* for  $\text{C}_{17}\text{H}_{22}\text{Cl}_2\text{MnN}_4$ : C, 50.02; H, 5.43; N, 13.72. Found: C, 50.02; H, 5.31; N, 13.24%.

**2.2.2.5.  $[\text{Mn}(\text{L5})\text{Cl}_2]$  (5).** This complex was prepared in a manner analogous to that described for **2** using L5 instead of L2. Colorless crystals suitable for X-ray diffraction were grown from a slow evaporation methanolic solution of the complex. Yield: 85%; *Anal. Calc.* for  $\text{C}_{18}\text{H}_{24}\text{Cl}_2\text{MnN}_4$ : C, 51.20; H, 5.73; N, 13.27. Found: C, 51.11; H, 5.54; N, 13.12%. ESI-MS of methanolic solution of **5** shows prominent peak at  $m/z$  values 386.2 and 410.1 (base peak) corresponding to  $[\text{Mn}(\text{L5})\text{Cl}]^+$  and  $[\text{Mn}(\text{L5})\text{Cl} + \text{Na}]^+$ , respectively.

## 2.3. Physical measurements

Elemental analyses were performed on a Perkin Elmer Series II CHNS/O analyzer 2400. The electronic spectra were recorded on an Agilent 8453 diode array spectrophotometer.  $^1\text{H}$  NMR spectra were recorded on a Bruker 400 MHz NMR spectrometer. GC–MS analysis was performed on Agilent GC–MS spectrometer using a HP-5 capillary column. All ligands were purified by using Teledyne Isco Combi Flash  $R_f$  flash chromatography. ESI mass spectra of the complexes were recorded with a Thermofinnigan LCQ-6000 Advantage Max ion trap mass spectrometer equipped with an electron spray source by using methanol as solvent. Cyclic voltammetry (CV) and differential pulse voltammetry (DPV) were performed using a three electrode cell configuration. A platinum sphere, a platinum plate and  $\text{Ag}(\text{s})/\text{Ag}^+$  were used as working, auxiliary, and reference electrodes, respectively. The supporting electrolyte used was  $\text{NBu}_4 \cdot \text{ClO}_4$  (TBAP). The temperature of the electrochemical cell was maintained at  $25.0 \pm 0.2$  °C by a cryocirculator (HAAKE D8 G). By bubbling research grade nitrogen, the solutions were deoxygenated and maintained under nitrogen atmosphere during measurements. The  $E_{1/2}$  values were observed under identical conditions for various scan rates. The instruments utilized included an EG & G PAR 273 Potentiostat/Galvanostat to carry out the experiments and to acquire the data. The products were quantified by using Hewlett Packard (HP) 6890 Gas Chromatograph (GC) series equipped with a FID detector and a HP-5 capillary column (30 m  $\times$  0.32 mm  $\times$  2.5  $\mu\text{m}$ ).

## 2.4. Reactivity studies

The catalytic activity of all the complexes towards cyclooctene, cyclohexene and styrene was examined by treating a solution of  $[\text{Mn}(\text{L1A-L5})(\text{Sol})_2]^{2+}$  prepared by treating the complexes  $[\text{Mn}(\text{L1A-L5})\text{Cl}_2]$  with two equivalents of  $\text{AgClO}_4$  dissolved in acetonitrile and centrifuging the solution to remove  $\text{AgCl}$ . The oxygenated products were identified by Agilent GC–MS instrument equipped with 7890A GC system 5975C MSD using a HP-5 capillary column and quantified by GC using Hewlett-Packed HP 6890 series gas chromatograph equipped with an FID detector and a HP-5 capillary column (30 m, 0.32 mm i.d) with the following temperature program: initial temperature, 80 °C, 5°  $\text{min}^{-1}$ ; final temperature 250 °C; detector temperature 250 °C.

## 2.5. Crystal data collection and structure refinement

Single crystal X-ray diffraction data for complexes **1**, **3A**, **4** and **5** were collected on a Bruker SMART Apex diffractometer equipped with a CCD area detector at 100 K with  $\text{Mo-K}\alpha$  ( $\lambda = 0.71073$  Å) radiation. A crystal of suitable size was immersed in paraffin oil and mounted on the tip of a glass fiber and cemented by using epoxy

resin. The crystallographic data and experimental parameters of the complexes **1**, **3A** and **5** are listed in Tables 1 and 4 in S1 respectively. For the data collection SAINT [37] software program was used for frames of data, indexing the reflections, and determination of lattice parameters; SAINT program for integration of the intensity of reflections and scaling. An empirical absorption correction was applied to the collected reflections with SADABS [38]. The structure was solved by direct methods using SHELXTL [39] and was refined on  $F^2$  by the full-matrix least-squares technique using the SHELXL-97 program package [40]. All non-hydrogen atoms were refined anisotropically till convergence was reached for the three complexes. Hydrogen atoms attached to the ligand moieties are either located from the difference Fourier map or stereochemically fixed. The crystallographic data and details of data collection for **1**, **3A** and **5** are given in Table 1.

### 3. Results and discussion

#### 3.1. Synthesis and characterization of ligands and complexes

The ligands L1 and L3 (Scheme 1) were synthesized according to a known two step procedure involving condensation of pyridine-2-carboxaldehyde with the corresponding alkylamines to form a Schiff base followed by ring closure with paraformaldehyde. The ligands L2 and L5 were prepared by reacting two equivalents of picolylchloride with piperazine and 1,5-diazacyclooctane, respectively. The ligand L4 was prepared by reductive amination of two equivalents of pyridine-2-carboxaldehyde with homopiperazine using sodium triacetoxyborohydride as reducing agent. The ligands were treated with equimolar amounts of  $\text{MnCl}_2 \cdot 4\text{H}_2\text{O}$  in methanol to give mononuclear Mn(II) complexes in good yields. All the complexes have been formulated as  $[\text{Mn}(\text{L})\text{Cl}_2]$  on the basis of elemental and ESI-MS analyses, which is supported by the X-ray structures of  $[\text{Mn}(\text{L4})\text{Cl}_2]$  **4** and  $[\text{Mn}(\text{L5})\text{Cl}_2]$  **5**. Interestingly, when the ligand L1 was treated with  $\text{MnCl}_2 \cdot \text{H}_2\text{O}$  and left to stand to obtain the complex  $[\text{Mn}(\text{L1})\text{Cl}_2]$ , only  $[\text{Mn}(\text{L1A})\text{Cl}_2]$  **1** was isolated. The imidazolidine ring of the linear tetradentate ligand L1 has undergone hydrolysis to form L1A in the presence of Mn(II) ion (cf. below). The complex isolated on treating  $[\text{Mn}(\text{L3})\text{Cl}_2]$  with  $\text{Ag}(\text{OTf})$  is formulated as

$[\text{Mn}(\text{L3})(\text{OTf})_2(\text{H}_2\text{O})]$  **3A**, which is supported by its X-ray structure. The divergent flexibility of the present tetradentate diaza ligands is expected to influence the coordination geometry as well as electronic properties of the complexes and confer a systematic variation in Lewis acidity of the Mn(II) center and hence provide a totally different communication to the substrate, oxidizing agent and dioxygen during oxygenation. The electronic absorption spectra of complexes **1–5** exhibit no Ligand Field band, which is expected of high-spin Mn(II). In frozen methanol solution all the complexes exhibit well-resolved six-line hyperfine EPR signals centered around  $g = 2.0$ , which is consistent with high-spin ( $S = 5/2$ ) Mn(II) species [17]. Typical spectra of complexes **1** and **3** are shown in Figs. S1 and S2. Conductivity measurements in acetonitrile ( $\Lambda_M$ ,  $6\text{--}15 \Omega^{-1} \text{cm}^2 \text{mol}^{-1}$ ) reveal that the complexes behave as non-electrolytes.[41].

#### 3.2. Description of molecular structure of $[\text{Mn}(\text{L1A})\text{Cl}_2]$ **1**, $[\text{Mn}(\text{L3})(\text{OTf})_2(\text{H}_2\text{O})]$ **3A**, $[\text{Mn}(\text{L4})\text{Cl}_2]$ **4** and $[\text{Mn}(\text{L5})\text{Cl}_2]$ **5**

The X-ray crystal structure of  $[\text{Mn}(\text{L1A})\text{Cl}_2]$  **1** is depicted in Fig. 1 together with atom numbering scheme. The selected bond distances and bond angles are collected in Table 2. The complex molecule possesses a distorted octahedral coordination geometry constituted by the two pyridine nitrogen atoms (N1, N4) and two tertiary amine nitrogen atoms (N2, N3) of the ligand L1A and two chloride ions completing the remaining *cis*-coordination sites *trans* to the two tertiary amine nitrogens. The linear tetradentate ligand adopts a *cis*- $\alpha$  mode of coordination around Mn(II) center with the two pyridine nitrogens *trans* to each other (Fig. 1). The bond angles of  $\text{N}(1)\text{--Mn}(1)\text{--N}(4)$  ( $162.70(18)^\circ$ ),  $\text{N}(3)\text{--Mn}(1)\text{--Cl}(1)$  ( $159.2(14)^\circ$ ) and  $\text{N}(2)\text{--Mn}(1)\text{--Cl}(2)$  ( $158.6(15)^\circ$ ) deviate markedly from the ideal octahedral bond angle of  $180^\circ$  indicating that the octahedral coordination geometry is distorted. The  $\text{Mn}\text{--N}_{\text{py}}$  bond ( $2.324(5)$ ,  $2.338(6)$  Å) in **1** is longer than that reported for  $[\text{Mn}(\text{BPMEN})\text{Cl}_2]$ , where BPMEN is *N,N'*-dimethyl-*N,N'*-bis(2-pyridylmethyl)-1,2-diaminoethane, with symmetrical Mn–N bonds ( $\text{Mn}\text{--N}_{\text{py}}$ ,  $2.272(2)$  Å) [33]. However, the  $\text{Mn}\text{--N}_{\text{amine}}$  bond ( $2.325(6)$ ,  $2.322(6)$  Å) in the former is shorter than that in  $[\text{Mn}(\text{BPMEN})\text{Cl}_2]$  revealing that the orientation of the nitrogen lone

**Table 1**  
Crystallographic data and structure refinement of **1**, **3A** and **5**.

	<b>1</b>	<b>3A</b>	<b>5</b>
Empirical formula	$\text{C}_{14}\text{H}_{18}\text{Cl}_2\text{MnN}_4$	$\text{C}_{18}\text{H}_{22}\text{F}_6\text{MnN}_4\text{O}_7\text{S}_2$	$\text{C}_{18}\text{H}_{24}\text{Cl}_2\text{MnN}_4$
Formula weight (g/mol)	368.16	637.44	422.25
Crystal color	colorless	colorless	colorless
Crystal system	monoclinic	monoclinic	monoclinic
Space group	$P21/c$	$P21/c$	$C2/c$
<i>a</i> (Å)	16.641(9)	19.7016(5)	22.6772(6)
<i>b</i> (Å)	8.115(4)	8.80609(2)	7.8471(2)
<i>c</i> (Å)	13.182(2)	15.7990(3)	13.8350(4)
$\alpha$ ( $^\circ$ )	90	90	90
$\beta$ ( $^\circ$ )	112.407(8)	103.122(1)	126.09(3)
$\gamma$ ( $^\circ$ )	90	90	90
<i>V</i> (Å <sup>3</sup> )	1645.7(15)	2669.43(10)	1989.30(12)
Residual electron density(max, min)	0.66, –0.51	0.31, –0.27	0.86, –0.89
<i>Z</i>	4	4	4
$\rho_{\text{calc}}$ (g/cm <sup>3</sup> )	1.486	1.591	1.410
<i>F</i> (000)	756	1300	876
<i>T</i> (K)	293	293	296
Number of reflections collected	3224	43340	21070
Number of unique reflections	3174	4947	2752
Radiation [Mo <i>K</i> $\alpha$ ] (Å)	0.71073	0.71073	0.71073
Residuals [ $I > 2\sigma(I)$ ]	1771	3864	2061
$R_1^a$	0.078	0.0360	0.0445
$wR_2^b$	0.2223	0.0995	0.1119

<sup>a</sup>  $R_1 = [\sum(|F_o| - |F_c|)] / \sum|F_o|$ .

<sup>b</sup>  $wR_2 = \{[\sum(w(F_o^2 - F_c^2)^2) / \sum(wF_o^4)]^{1/2}\}$ .

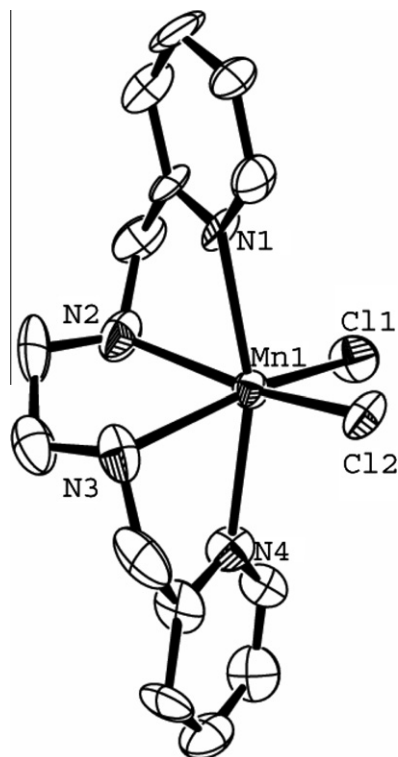


**Fig. 1.** ORTEP diagram of **1** showing 40% probability thermal ellipsoids and the labeling scheme for selected atoms. All of the hydrogen atoms are omitted for clarity.

pair orbital towards the Mn(II) center in the latter deviates upon incorporation of methyl groups. The X-ray crystal structure of  $[\text{Mn}(\text{L3})(\text{OTf})_2(\text{H}_2\text{O})]$  **3A** is depicted in Fig. 2 together with atom numbering scheme, and the selected bond distances and bond angles are collected in Table 2. The Mn(II) center in **3A** adopts a rare distorted pentagonal bipyramidal coordination geometry. The corners of the distorted pentagonal plane of the coordination polyhedron are occupied by three nitrogen atoms (N2, N3, N4) of the ligand L3, and the oxygen atoms of triflate anion (O2) and water molecule (O3). The axial positions are occupied by the N(1) nitrogen of L3 and the oxygen atom O(1) of triflate anion with the N(1)–Mn(1)–O(1) bond angle being  $169.53^\circ$ . The Mn–N<sub>amine</sub> bond (2.362(3), 2.411(2) Å) is longer than the Mn–N<sub>py</sub> bond (2.290(2), 2.323(2) Å) due to  $sp^3$  and  $sp^2$  hybridizations respectively of the amine and pyridine nitrogen atoms [42]. The equatorial triflate anion displays a weaker interaction with the Mn(II) center than the axial one (Mn–O2, 2.360, Mn–O1, 2.222 Å), obviously due to steric crowding in the equatorial plane. Out of the five equatorial bond angles the three bond angles N(2)–Mn(1)–O(2) ( $165.58^\circ$ ), N(4)–Mn(1)–O(3) ( $150.02^\circ$ ) and N(2)–Mn(1)–N(3) ( $111.78^\circ$ ) deviate significantly from the ideal value ( $72^\circ$ ) of the pentagonal bipyramidal geometry, presumably because of unfavorable steric interactions that would occur between the two tertiary amine nitrogens leading to strong distortion in the coordination geometry, and a chair conformation for the propylene moieties of the diazacycloalkane ligand backbone (Fig. 2).

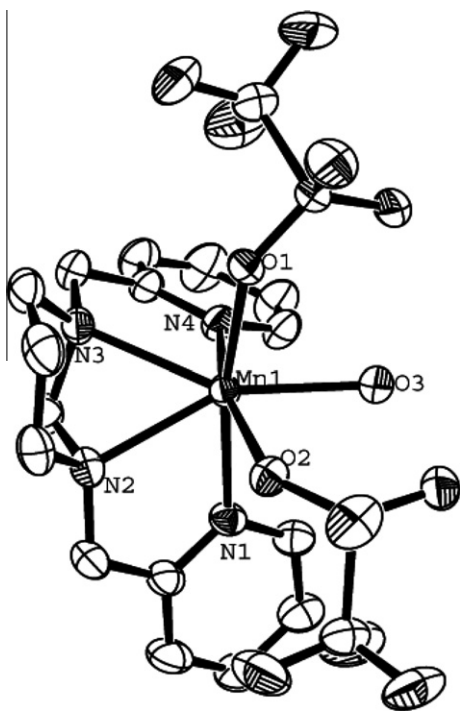
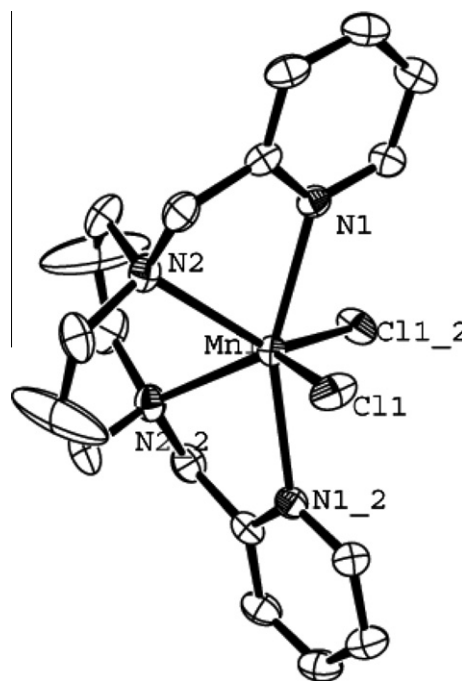
The crystal data for the complex  $[\text{Mn}(\text{L4})\text{Cl}_2]$  **4** are presented in Table S1 and the ORTEP diagram along with atom numbering scheme is presented in Fig. S3. As the R value of the structure is high, only the geometry of the complex is discussed in comparison with those of related complexes. The complex molecule exhibits a distorted octahedral geometry around Mn(II) and the linear tetradentate ligand L4 adopts a *cis- $\alpha$*  mode of coordination leading to

the orientation of two pyridine nitrogens *trans* to each other and the chloride ions *cis* to each other. Such a geometry is similar to that observed in  $[\text{Mn}(\text{BPMEN})\text{Cl}_2]$ , a linear 4N ligand like L4 [33], but different from the seven-coordinate distorted pentagonal bipyramidal geometry [43] of the complex ion  $[\text{Mn}(\text{L4})(\text{CH}_3\text{CN})_3]^{2+}$  in which the same ligand defines the quite ruffled equatorial plane and three  $\text{CH}_3\text{CN}$  solvent molecules complete the seven-coordinate structure. The ability of the L4 ligand to occupy the equatorial plane is evident also in the square pyramidal complex [35]  $[\text{Cu}(\text{L4})(\text{ClO}_4)]^+$ . Interestingly, the *in situ* generated complex  $[\text{Fe}(\text{L4})(\text{CH}_3\text{CN})_3]^{2+}$  also had been predicted [44] to contain the ligand in the equatorial plane with the two chloride ions coordinated *trans* to each other. Interestingly, in the tetrachlorocatechol adduct of the iron(III) complex  $[\text{Fe}(\text{L4})(\text{cat})]^+$  the ligand is bound in a *cis- $\beta$*  orientation [36]. Thus it is evident that the sterically unnumbered ligand L4 is capable of assuming any orientation, *cis- $\alpha$*  or *cis- $\beta$* , depending on the ligand donor atoms. Interestingly, the propylene chain in **4** adopts a chair rather than boat conformation to minimize the steric interactions caused by the propylene and ethylene moieties of L4 ligand (Fig. S3). Molecular model building studies of **4** reveal that the unfavorable steric interactions occurring between the propylene chain of the macrocyclic ligand backbone and the two chloride ions in *trans* positions force the ligand to adopt the *cis- $\alpha$*  mode of coordination geometry.

The X-ray crystal structure of  $[\text{Mn}(\text{L5})\text{Cl}_2]$  **5** is depicted in Fig. 3 together with atom numbering scheme. The selected bond distances and bond angles are collected in Table 2. The complex molecule possesses an uncommon distorted trigonal prismatic geometry with one of the trigonal faces (N(1)–N(2)–N(1\_2)) constituted by the two pyridine (N(1), N(2)) and one amine (N(1\_2)) nitrogen atoms of the tetradentate ligand and the other trigonal face (Cl(1)–Cl(1\_2)–N(2\_2)) opposite to it is constituted by the remaining amine nitrogen (N(2\_2)) atom of the ligand and two chloride ions (Cl(1), Cl(1\_2)). The lengths of the sides of the triangle N(1)–N(2)–N(1\_2) lie in the range 2.731(2)–4.630(3) Å while those of the triangle Cl(1)–Cl(1\_2)–N(2\_2) in the range 3.490(2)–4.438(3) Å, and the angles of both the triangles fall in the range  $35.35(7)$ – $78.80(7)^\circ$ . The torsion angles about the centroid of the triangular faces deviate markedly from the ideal angle of  $0^\circ$  indicating that the triangular faces are not exactly parallel to each other illustrating that the prismatic coordination environment around Mn(II) is distorted. The Mn–N<sub>amine</sub> (2.386(3) Å), Mn–N<sub>py</sub> (2.361(2) Å) and the Mn–Cl bonds (Mn(1)–Cl(1), 2.463(8) Å) are equal among themselves, which is expected of the  $C_2$  axis of symmetry and thus the respective pyridine nitrogens, amine nitrogens and chloride ions are symmetry related (Table 2). The Mn–N<sub>amine</sub> bond (2.386(3) Å) is longer than the Mn–N<sub>py</sub> bond (2.361(2) Å) due to  $sp^3$  and  $sp^2$  hybridizations respectively of the amine and pyridine nitrogen atoms [42]. As expected [45], the Mn–N<sub>py</sub>, Mn–N<sub>amine</sub> and Mn–Cl bond lengths are longer than the respective Fe–N<sub>py</sub> (2.305(2) Å), Fe–N<sub>amine</sub> (2.334(2) Å) and Fe–Cl (2.428(2) Å) bond lengths in the analogous iron(II) complex  $[\text{Fe}(\text{L5})\text{Cl}_2]$  with a similar distorted prismatic geometry [46]. Also, the chelate ring in the iron(II) complex is in a chair conformation but that in the Mn(II) analog is a flattened chair indicating the strong steric clash between the two propylene groups, which is avoided in the prismatic geometry by the flattening of the chelate ring. Upon incorporating a methylene group in between  $-\text{CH}_2-$  groups in the diazacycloalkane ligand in **4** to obtain **5** the distorted octahedral geometry in both *cis- $\alpha$*  and *trans* mode of coordination becomes unstable due to unfavorable steric interactions between the six-membered chelate ring in **5** and leads to form the uncommon trigonal prismatic geometry. Molecular model building studies reveal that the steric interactions caused between the two propylene chains and also with the central metal atom both in

**Table 2**  
Selected bond lengths (Å) and bond angles (°) for [Mn(L1A)Cl<sub>2</sub>] **1**, [Mn(L3)(H<sub>2</sub>O)(CF<sub>3</sub>SO<sub>3</sub>)<sub>2</sub>] **3A** and [Mn(L5)Cl<sub>2</sub>] **5**.

<b>1</b>		<b>3A</b>		<b>5</b>	
Mn(1)–N(1)	2.324(3)	Mn(1)–N(1)	2.290(2)	Mn(1)–N(1)	2.361(2)
Mn(1)–N(2)	2.332(5)	Mn(1)–N(2)	2.362(3)	Mn(1)–N(2)	2.386(3)
Mn(1)–N(3)	2.328(6)	Mn(1)–N(3)	2.411(2)	Mn(1)–N(2_2)	2.386(3)
Mn(1)–N(4)	2.338(5)	Mn(1)–N(4)	2.323(2)	Mn(1)–N(1_2)	2.361(2)
Mn(1)–Cl(1)	2.449(2)	Mn(1)–O(1)	2.222(18)	Mn(1)–Cl(1)	2.463(8)
Mn(1)–Cl(2)	2.454(19)	Mn(1)–O(2)	2.360(19)	Mn(1)–Cl(1_2)	2.463(8)
		Mn(1)–O(3)	2.259(2)		
N(1)–Mn(1)–N(2)	71.16(18)	O(1)–Mn(1)–O(2)	88.10(7)	Cl(1)–Mn(1)–N(1)	84.54(6)
N(1)–Mn(1)–N(3)	94.85(2)	O(1)–Mn(1)–O(3)	83.80(7)	Cl(1)–Mn(1)–N(2)	92.06(7)
N(1)–Mn(1)–N(4)	162.70(18)	O(1)–Mn(1)–N(1)	169.53(7)	Cl(1)–Mn(1)–Cl(1_2)	126.39(3)
N(2)–Mn(1)–N(3)	76.0(2)	O(1)–Mn(1)–N(2)	95.97(7)	Cl(1)–Mn(1)–N(1_2)	85.34(7)
N(2)–Mn(1)–N(4)	95.41(2)	O(1)–Mn(1)–N(3)	114.53(8)	Cl(1)–Mn(1)–N(2_2)	132.51(7)
N(3)–Mn(1)–N(4)	70.77(2)	O(1)–Mn(1)–N(4)	81.28(7)	N(1)–Mn(1)–N(2)	70.25(8)
Cl(1)–Mn(1)–Cl(2)	103.39(7)	O(2)–Mn(1)–O(3)	81.16(8)	Cl(1_2)–Mn(1)–N(1)	85.34(7)
Cl(1)–Mn(1)–N(1)	98.04(15)	O(2)–Mn(1)–N(1)	84.51(7)	N(1)–Mn(1)–N(1_2)	57.43(8)
Cl(1)–Mn(1)–N(2)	92.74(17)	O(2)–Mn(1)–N(2)	165.58(7)	N(1)–Mn(1)–N(2_2)	130.29(8)
Cl(1)–Mn(1)–N(3)	159.20(14)	O(2)–Mn(1)–N(3)	78.66(8)	Cl(1_2)–Mn(1)–N(2)	132.51(7)
Cl(2)–Mn(1)–N(4)	93.35(15)	O(2)–Mn(1)–N(4)	123.95(7)	N(1_2)–Mn(1)–N(2)	130.29(8)
Cl(2)–Mn(1)–N(1)	92.52(12)	O(3)–Mn(1)–N(1)	87.74(8)	N(2)–Mn(1)–N(2_2)	75.83(9)
Cl(2)–Mn(1)–N(2)	158.65(15)	O(3)–Mn(1)–N(2)	85.53(8)	Cl(1_2)–Mn(1)–(1_2)	84.54(6)
Cl(2)–Mn(1)–N(3)	92.23(15)	O(3)–Mn(1)–N(3)	152.01(9)	Cl(1_2)–Mn(1)–(2_2)	92.06(7)
Cl(2)–Mn(1)–N(4)	97.48(14)	O(3)–Mn(1)–N(4)	150.02(9)		
		N(1)–Mn(1)–N(2)	89.48(8)		
		N(1)–Mn(1)–N(3)	71.25(8)		
		N(1)–Mn(1)–N(4)	109.02(7)		
		N(2)–Mn(1)–N(3)	111.78(8)		
		N(2)–Mn(1)–N(4)	70.42(8)		
		N(3)–Mn(1)–N(4)	57.52(8)		

**Fig. 2.** ORTEP diagram of **3A** showing 30% probability thermal ellipsoids and the labeling scheme for selected atoms. All of the hydrogen atoms are omitted for clarity.**Fig. 3.** ORTEP diagram of **5** showing 30% probability thermal ellipsoids and the labeling scheme for selected atoms. All of the hydrogen atoms are omitted for clarity.

chair and boat conformations in octahedral coordination geometry forces **5** to adopt the trigonal prismatic geometry.

For all the complexes, the observed Mn(II)–ligand bond lengths range from 2.1 to 2.5 Å, which is expected for the high-spin Mn(II) center. Upon connecting the two methyl groups in [Mn(BPMEN)Cl<sub>2</sub>] to form an ethylene linkage as in [Mn(L2)(CH<sub>3</sub>CN)<sub>3</sub>]<sup>2+</sup> and a propyl-

ene linkage as in [Mn(L4)(CH<sub>3</sub>CN)<sub>3</sub>]<sup>2+</sup> both the Mn–N<sub>py</sub> bond distances increase with the Mn–N<sub>amine</sub> bond distances remaining almost constant [43]. As expected, on replacing the ethylene in the ligand diazacycloalkane backbone of **4** by a methylene to obtain **3** both the Mn–N<sub>amine</sub> and Mn–N<sub>py</sub> bond distances increase leading to enhancement in Lewis acidity of the Mn(II) center. Further, upon

enlarging the ethylene linkage in **4** into propylene linkage as in **5** the Mn–N<sub>py</sub> and Mn–N<sub>amine</sub> bond distances increase resulting in a similar enhancement in Lewis acidity of the Mn(II) center. Thus it is evident that changes in variation of ligand diazacycloalkane backbone leads to variation in Lewis acidity of the Mn(II) center. This effect is reflected in the Mn(II)/Mn(III) redox potential of the complexes (cf. below).

### 3.3. Manganese(II) promoted hydrolysis of imidazolidine ring

In solution the ligand L1 undergoes imidazolidine ring-cleavage reaction in the presence of Mn(II) ion. Ray et al. have reported that the binucleating ligand 2-phenyl-1,3-bis[3'-aza-4'-(2'-hydroxyphenyl)-prop-4-en-1'-yl]-1,3-imidazolidine bound to Mn(II) or Fe(III) undergoes imidazolidine ring hydrolysis with the expulsion of one mole of aldehyde [47]. We propose that coordination of Mn(II) to L1 with the highly strained imidazolidine ring on its backbone leads to activation of the methylene carbon flanked by two coordinated amine nitrogen atoms, followed by nucleophilic attack by a water molecule leading to the formation of imidazolidine ring hydrolyzed complex **1**. However, **3** with a methylene group also flanked by two coordinated amine nitrogen atoms is stable towards such hydrolysis. This illustrates that it is the ethylene linker between the amine nitrogens which tends to confer steric congestion on the coordinated L1 ligand leading to the activation of methylene group towards hydrolysis.

### 3.4. Electrochemical behavior

The electrochemical features of the Mn(II) complexes, except **2**, were investigated in acetonitrile solution by employing cyclic (CV) and differential pulse voltammetry (DPV) on a stationary platinum-sphere electrode. The poor solubility of **2** in acetonitrile limited the study of its electrochemical behavior. Typical cyclic and differential pulse voltammograms of complexes are depicted in Figs. 4 and S4–S6. The Mn(II)/Mn(III) redox potentials ( $E_{1/2}$ , Table 3) follow the trend **1** < **4** < **3** < **5**, reflecting the increase in Lewis acidity of the Mn(II) center from left to right along the series.

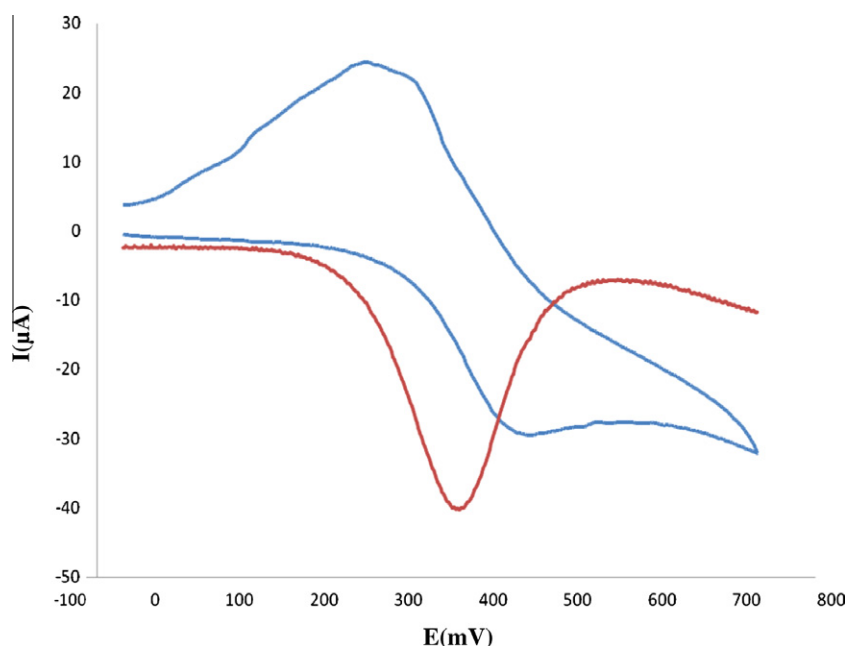


Fig. 4. Cyclic (CV) and differential pulse voltammograms (DPV) of [Mn(L1A)Cl<sub>2</sub>] **1** in acetonitrile solution at 25 °C. Supporting electrolyte: 0.1 M TBAP. Scan rate: 50 mV s<sup>-1</sup> for CV and 5 mV s<sup>-1</sup> for DPV.

The Mn(II)/Mn(III) redox potential of [Mn(L1A)Cl<sub>2</sub>] **1** is less positive than that of [Mn(BPMEN)Cl<sub>2</sub>] (0.740 V versus SCE) [33], where BPMEN is the *N,N'*-dimethyl analog of L1A, illustrating that *N*-methylation leads to improper orientation of the amine nitrogen lone pair towards Mn(II) orbital. A similar observation has been made earlier for the iron(III) complexes of 3N ligands with *N*-alkyl substituents [48]. Upon incorporating a propylene bridge in between the amine nitrogens in [Mn(L1A)Cl<sub>2</sub>] **1** to obtain **4**, the Mn(II)/Mn(III) redox potential becomes more positive suggesting a similar improper orientation of the lone pair orbitals towards Mn(II). Also, upon replacing the ethylene bridge in **4** by a methylene bridge to obtain **3** the lone pair orbitals on the amine nitrogen atoms in the latter deviate further from exact orientation towards Mn(II) orbitals leading to a higher Lewis acidity of Mn(II) center and hence a higher Mn(II)/Mn(III) redox potential for **3**. Similarly, upon replacing the ethylene bridge in **4** by a propylene bridge as in **5** the lone pair orbitals on the amine nitrogen atoms in the latter deviate much from exact orientation towards Mn(II) orbitals leading to increased positive charge on Mn(II) center and hence the higher Mn(II)/Mn(III) redox potential of **5**. In other words, upon increasing the size of the diazacycloalkane ring in the ligand backbone on going from **4** to **5**, and enhancing the steric crowding around the metal center on going from **4** to **3** the Lewis acidity of the Mn(II) center increases leading to significant variation in the Mn(II)/Mn(III) redox potential.

### 3.5. Catalytic properties

The catalytic activity of complexes **1–5** towards olefin epoxidation was investigated by using PhIO as the oxygen source. All the reactions were performed at least thrice, and the amounts of products reported represent the average obtained. In these reactions 1 equiv. of the complex, 100 equiv. of PhIO, 500 equiv. of both the olefin substrate and decane (internal standard) are typically mixed in acetonitrile. The solution was stirred for 1 h at room temperature under nitrogen atmosphere and then passed through a silica column. The resulting solution was directly analyzed by GC and GC–MS. The yields of products were determined by

**Table 3**

Electrochemical data<sup>a</sup> of mononuclear Mn(II) complexes in acetonitrile solution at 25 ± 0.2 °C.

Complex	$E_{p,a}$ (V)	$E_{p,c}$ (V)	$\delta E_p$ (V)	$E_{1/2}$ (V)		Redox process
				CV	DPV	
[Mn(L1A)Cl <sub>2</sub> ]	0.468	0.307	0.160	0.387	0.389	Mn <sup>II</sup> → Mn <sup>III</sup>
[Mn(L3)Cl <sub>2</sub> ]	0.897	0.783	0.114	0.840	–	Mn <sup>II</sup> → Mn <sup>III</sup>
[Mn(L4)Cl <sub>2</sub> ]	0.626	0.478	0.148	0.552	0.553	Mn <sup>II</sup> → Mn <sup>III</sup>
[Mn(L5)Cl <sub>2</sub> ]	–	–	–	–	0.863	Mn <sup>II</sup> → Mn <sup>III</sup>

<sup>a</sup> Potential measured (±0.002 V) vs. Ag(s)/Ag<sup>+</sup> (0.01 M, 0.10 M TBAP); add 0.544 V to convert to NHE.

comparison of peak area with those of known authentic samples. All the chloride complexes show very low yield (<5%) under these conditions. When the solvent coordinated species [Mn(L)(CH<sub>3</sub>CN)<sub>2</sub>]<sup>2+</sup> generated by treating the complexes with silver perchlorate in acetonitrile solution to remove the coordinated chloride ions (cf. above) was used as the catalyst, the catalytic activity observed within 1 h (Tables 4 and 5, Scheme 2) is significantly high in comparison to MnCl<sub>2</sub> and Mn(ClO<sub>4</sub>)<sub>2</sub>, which are poor catalysts under the same experimental conditions. This illustrates that the coordinated chloride ions in the complexes are difficult to be displaced to obtain the reactive Mn(II) complex species. The encouraging yields observed for the epoxidation of *cis*-cyclooctene by using the solvated complexes prompted us to improve the yield by optimizing the reaction conditions in terms of solvent, temperature and different additives. The influence of solvent on epoxidation was explored by carrying out the reactions in different solvents like methanol, dichloromethane and acetonitrile, and as expected [49], the highest activity (results are not shown here) is achieved in acetonitrile as solvent. It has been shown that when a mixture of the ligand L1 and Mn(ClO<sub>4</sub>)<sub>2</sub>·6H<sub>2</sub>O was reacted with H<sub>2</sub>O<sub>2</sub> as oxidant in the presence of a mild base like NaOAc in acetone solvent at 0 °C over 16 hours the pyridyl moiety of the ligand underwent oxidative degradation leading to the formation of picolinic acid, which in the presence of the Mn(II) salt catalyzes the

epoxide formation [19]. However, when control experiments were performed for the solvated complexes at room temperature using 1 equiv. of the complex and 100 equiv. of PhIO in the absence of the substrate in acetonitrile solvent and the products analyzed, no picolinic acid formation was detected. So it is evident that the pyridyl moieties of **1–5** do not undergo any oxidative degradation under the present catalytic reaction conditions.

The epoxidation of *cis*-cyclooctene catalyzed by [Mn(L)(CH<sub>3</sub>CN)<sub>2</sub>]<sup>2+</sup> species proceeds with both conversion (21–54%) and selectivity (100%) for *cis*-epoxide higher than those previously reported [21] for the Mn(II) complexes of linear 4N ligands such as [Mn(BPMEN)(CF<sub>3</sub>SO<sub>3</sub>)<sub>2</sub>] and [Mn(BPMCN)(CF<sub>3</sub>SO<sub>3</sub>)<sub>2</sub>], where BPMCN is *N,N*-dimethyl-*N,N*-bis(2-pyridylmethyl)cyclohexane-(1*R*,2*R*)-diaminoethane, which exhibit conversions of only 35% and 24%, respectively. Among the present complexes, the yield of epoxidation product *cis*-cyclooctene oxide follows the trend, **1** > **4** > **5** ≈ **2** > **3**. Among **1**, **3**, **4** and **5** with the same octahedral coordination geometry, the complex **1** possesses the highest reactivity. Upon incorporating the diazacycloalkane ring in **1** to obtain **4**, and upon replacing the ethylene bridge in **4** by a propylene bridge to obtain **5**, the Lewis acidity of the Mn(II) center increases, as evident from the increase in Mn(II)/Mn(III) redox potential along the above series (cf. above), leading to a decrease in ease of generating the high-valent oxo intermediate, and hence the decrease in the epoxide yield along the above series. Similarly, upon replacing the ethylene bridge in **4** by a methylene bridge as in **3** enormous steric congestion is caused in the diazacycloalkane backbone, the redox potential of the latter becomes higher than the former resulting in a lower epoxidation activity for the latter; however, **3** shows an activity lower than **5**, possibly because the diazacycloalkane backbone with enormous steric congestion discourages the formation of the high-valent oxo species involved in catalysis. This also illustrates the same trend in epoxidation activity of the Mn(II) complexes towards cyclohexene and styrene.

Upon adding 2 equiv. of *N*-methylimidazole (*N*-Melm) as additive the product conversion increases from 20–54% to 23–64%,

**Table 4**

Epoxidation<sup>a</sup> of cyclooctene, cyclohexene and styrene catalyzed by Mn(II) complexes<sup>c</sup> using PhIO in acetonitrile.

Complex	Cyclooctene <sup>b</sup>		Cyclohexene <sup>b</sup>				Styrene <sup>b</sup>		
	-oxide	Selectivity (%)	-oxide	-ol	-one	Selectivity (%)	-oxide	Benzaldehyde	Selectivity (%)
Mn(ClO <sub>4</sub> ) <sub>2</sub> ·6H <sub>2</sub> O	<5	100	5.3	4.2	3.6	40.5	15.6	12.8	54.9
[Mn(L1A)(ACN) <sub>2</sub> ] <sup>2+</sup>	54	100	22.5	13.5	38.1	30.3	23.0	12.7	64.4
[Mn(L2)(ACN) <sub>2</sub> ] <sup>2+</sup>	20.6	100	12.0	12.2	41.0	18.0	17.0	11.2	60.2
[Mn(L3)(ACN) <sub>2</sub> ] <sup>2+</sup>	17.4	100	14.7	8.7	29.5	27.7	21.5	16.0	57.3
[Mn(L4)(ACN) <sub>2</sub> ] <sup>2+</sup>	33.1	100	18.5	17.0	52.1	18.0	46.8	13.9	77.1
[Mn(L5)(ACN) <sub>2</sub> ] <sup>2+</sup>	20.5	100	16.5	14.4	53.3	21.6	30	18.3	62.1

<sup>a</sup> Conditions: ratio of catalyst:PhIO:substrate = 1:100:500 in acetonitrile.

<sup>b</sup> Reaction mixtures were stirred for 1 h; yields based on oxidant used.

<sup>c</sup> [Mn(L)(ACN)<sub>2</sub>]<sup>2+</sup> generated by treating the complexes with silver perchlorate in acetonitrile.

**Table 5**

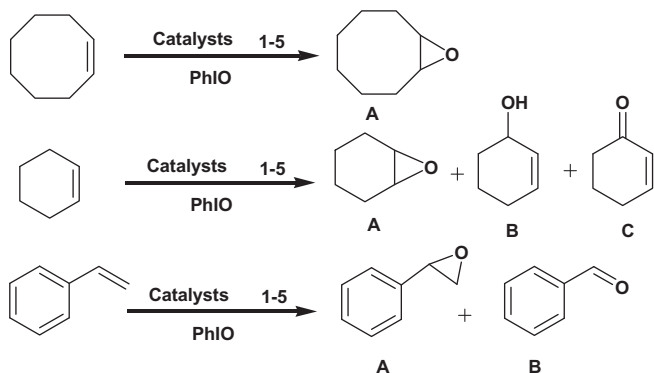
Epoxidation<sup>a</sup> of cyclooctene, cyclohexene and styrene catalyzed by Mn(II) complexes<sup>c</sup> with *N*-methyl imidazole additive using PhIO in acetonitrile.

Complex	Cyclooctene <sup>b</sup>		Cyclohexene <sup>b</sup>				Styrene <sup>b</sup>		
	-oxide	Selectivity (%)	-oxide	-ol	-one	Selectivity (%)	-oxide	Benzaldehyde	Selectivity (%)
Mn(ClO <sub>4</sub> ) <sub>2</sub> ·6H <sub>2</sub> O	<5	100	17.6	10.2	43.9	24.5	9.0	16.3	35.3
[Mn(L1A)(ACN) <sub>2</sub> ] <sup>2+</sup>	63.9	100	33.2	8	26.2	49.2	46.2	16.0	74.2
[Mn(L2)(ACN) <sub>2</sub> ] <sup>2+</sup>	28.3	100	16.4	7.9	28.4	31.1	26.4	12.1	64.9
[Mn(L3)(ACN) <sub>2</sub> ] <sup>2+</sup>	25.7	100	18.9	8.4	20.1	39.8	31.3	18.6	62.7
[Mn(L4)(ACN) <sub>2</sub> ] <sup>2+</sup>	42.7	100	28.0	8.0	24.2	46.5	46.5	13.9	76.9
[Mn(L5)(ACN) <sub>2</sub> ] <sup>2+</sup>	22.4	100	18.3	8.5	24.6	35.6	36.4	17.9	67.0

<sup>a</sup> Conditions: ratio of catalyst:*N*-methyl imidazole:PhIO: substrate = 1:2:100:500 in acetonitrile.

<sup>b</sup> Reaction mixtures were stirred for 1 h; yields based on oxidant used.

<sup>c</sup> [Mn(L)(ACN)<sub>2</sub>]<sup>2+</sup> generated by treating the complexes with silver perchlorate in acetonitrile.



**Scheme 2.** Epoxidation of alkenes by Mn(II) complexes.

and, interestingly, the product yield follows the same trend observed in the absence of added base,  $1 > 4 > 5 \approx 2 > 3$ . At high concentrations the coordination of monodentate *N*-Melm increases the electron density on Mn(II) center leading to stabilize the high-valent manganese-oxo species  $(4N)Mn^{IV}=O$ , which has been proposed as the active intermediates for oxygen transfer reactions. These species have been characterized by using various spectroscopic methods, and the DFT calculations confirm that this species is indeed energetically accessible and a few of these oxo-manganese(IV) compounds have been isolated successfully [30]. However, attempts to spectroscopically detect the catalyst-PhIO adduct species or the high-valent manganese-oxo intermediate by reacting the present complex species  $[Mn(L)(CH_3CN)_2]^{2+}$  with PhIO even at low-temperature ( $-40^\circ C$ ) were unsuccessful revealing their low stability. At higher concentrations of the added base the product yield decreases as the additive competes for the coordination geometry around the metal center, and discourages the binding of the oxidant to Mn(II) center. Similar *N*-Melm effects have been observed for Mn(III)-salen [50] and metalloporphyrin [51] catalyzed olefin epoxidation. The frozen solution EPR spectra of the reaction mixture obtained after completion of catalytic oxidation reaction show signals (Fig. S7) characteristic of high-spin Mn(II), revealing that the catalyst does not undergo any oxidative degradation. Based upon these observations we propose a bifurcated reaction mechanism: In one mechanism, the manganese-oxo intermediate, formed by the interaction of the catalyst with PhIO (Scheme 3A), attacks the olefinic double bond in a concerted pathway, which is similar to the one involving (salen) $Mn^V=O$  intermediate proposed [24] for the epoxidation reactions using

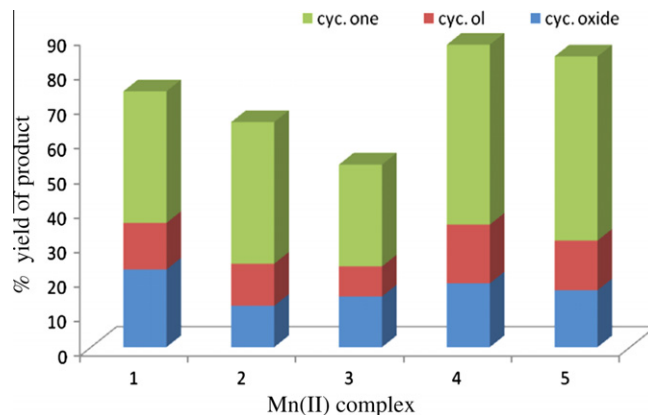
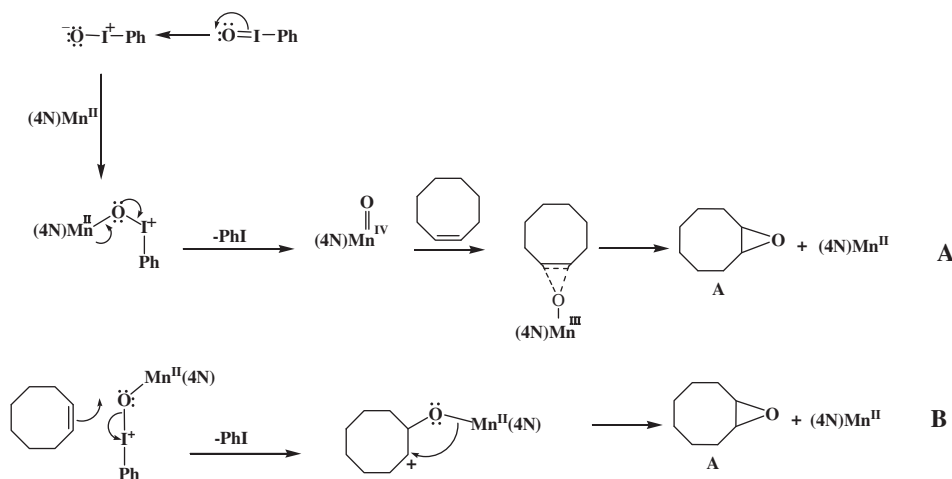


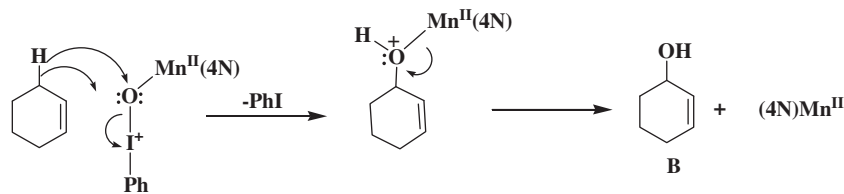
**Fig. 5.** Bar chart representation of cyclohexene epoxidation catalyzed by Mn(II) complexes (1–5) in the presence of PhIO at room temperature in acetonitrile.

Mn(III)-salen complexes and PhIO. In the other mechanism, the intermediate species  $[(4N)Mn-O-I^+-Ph]$ , which is similar to the one proposed for the epoxidation reactions using Mn(III)-salen complexes and iodoarenes [52], attacks cyclooctene directly to form the carbo cation  $[(4N)Mn-O-C_8H_{14}]^+$ , which collapses to give the epoxide product and regenerates the original complex (Scheme 3B). In fact, we have elegantly shown [53] that the intermediate peroxido species  $[Cl(ntb)Ru-O-O-tBu]^+$ , detected by ESI-MS, attacks the olefin directly to form the epoxide, without invoking the formation and involvement of the high-valent  $[(ntb)Ru^{IV}=O]$  species. It may be noted that the in-cage electronic rearrangement in the carbo cation is facilitated by a more Lewis basic ligand. Thus, as one moves from 1 to 4 to 5 the Lewis acidity of the Mn(II) center increases, and hence the ligand Lewis basicity decreases from L1 to L4 to L5 (or L3) resulting in the decrease in yield of the epoxide product, supporting our proposal. Thus the catalytic activity of the metal complex is controlled and tuned by the ligand electronic as well as steric factors imposed on the metal center. It would be interesting to study the use of the present catalysts for epoxidation of chiral alkenes, which would throw light on the reaction mechanism.

The epoxidation of cyclohexene has been also studied in acetonitrile solvent at room temperature using 1–5 as catalysts and PhIO as oxygen source under nitrogen atmosphere. In the epoxidation of cyclohexene, the major product observed is cyclohexene oxide (E, 17–23%, Table 4, Fig. 5), apart from allylic oxidation products like



**Scheme 3.** Proposed mechanisms for epoxidation of cyclooctene by using Mn(II) complexes and PhIO.



**Scheme 4.** Proposed mechanism for allylic oxidation of cyclohexene by using Mn(II) complexes and PhIO.

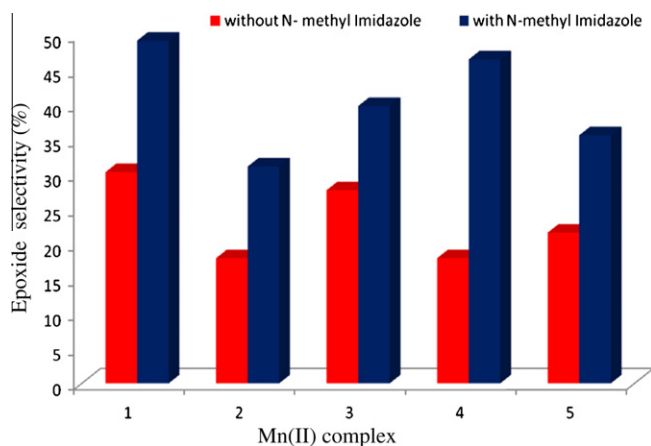


**Fig. 6.** Bar chart representation of selectivity catalyzed by Mn(II) complexes in ACN (1–5). Epoxide selectivity of cyclohexene in the presence and absence of additive (*N*-methyl imidazole).

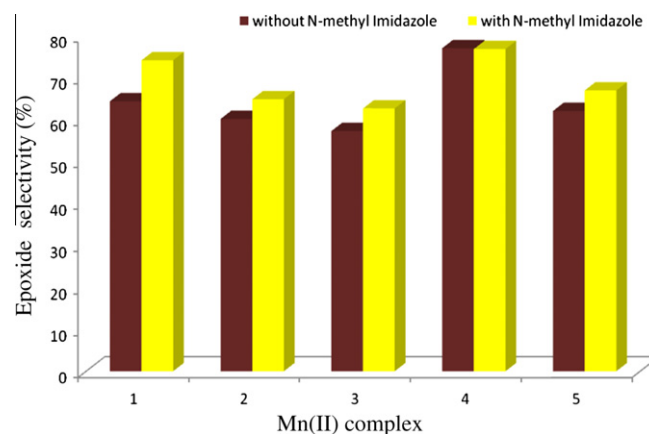


**Fig. 8.** Bar chart representation of selectivity catalyzed by Mn(II) complexes in ACN (1–5). Epoxide selectivity of styrene in the presence and absence of additive (*N*-methyl imidazole).

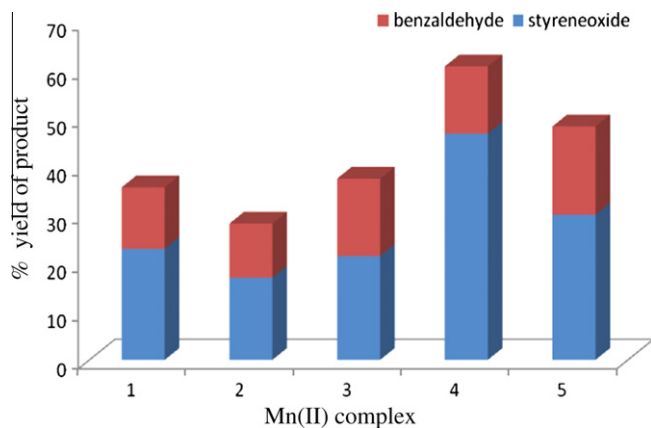


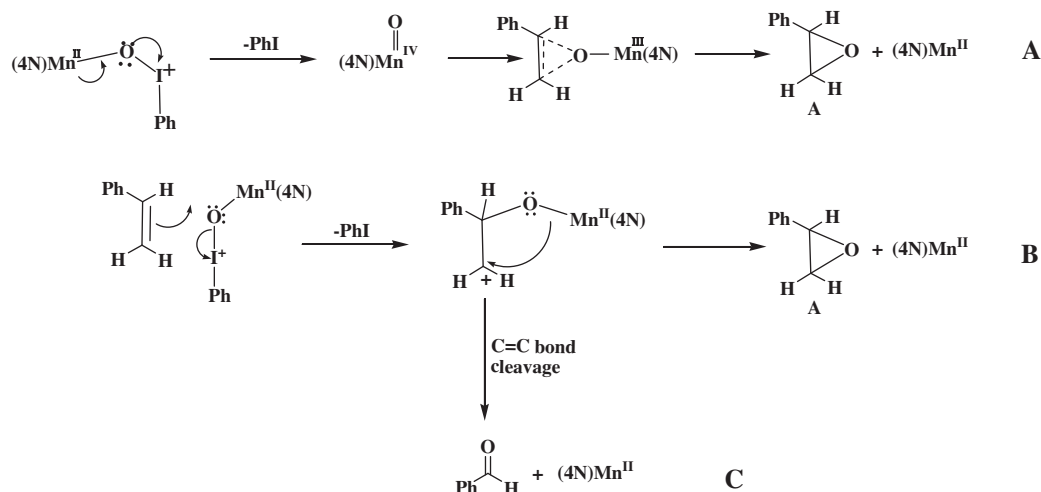
**Fig. 7.** Bar chart representation of styrene epoxidation catalyzed by Mn(II) complexes (1–5) in the presence of PhIO at room temperature in acetonitrile.

2-cyclohexen-1-ol and 2-cyclohexen-1-one, which is the further oxidized product of the former involving an oxidative dehydrogenation pathway [54] catalyzed by the complexes. The mechanism of epoxidation of cyclohexene is illustrated by invoking the involvement of  $[(4N)Mn-O-I^+-Ph]$  and the high-valent  $(4N)Mn^{IV}=O$  intermediate proposed above for the cyclooctene epoxidation (Scheme 3A and B). The formation of increased allylic oxidation products and decreased epoxide (*A/E*, 2.2–4.1), which is similar to that observed previously for  $Ru^{II}$  [54],  $Mn^{III}$  and  $Fe^{III}$  complexes [55], is illustrated by invoking the facile abstraction of allylic proton by  $[(4N)Mn-O-I^+-Ph]$  or the intermediate species  $(4N)Mn^{IV}=O$ , followed by in-cage electron-transfer to form the allylic alcohol product (Scheme 4).

The lower selectivity observed for 1–5 is due to the preferential attack of the allylic C–H bond rather than the olefinic double bond by  $[(4N)Mn-O-I^+-Ph]$  and  $(4N)Mn^{IV}=O$  species, which is similar to the reactive intermediate [54]  $(4N)Ru^{IV}=O$ . Control experiments for cyclohexene oxidation without the catalyst gave a total yield of only <8% under aerobic conditions, which is higher than the total yield of <2% obtained under anaerobic ( $N_2$ ) conditions for the same reaction, revealing the contribution of autooxidation of cyclohexene in the presence of oxygen, occurring through a free radical chain mechanism [56].

In the presence of *N*-methylimidazole, the epoxide yield increases with the product conversion increasing from 30% to 50% and the selectivity (*A/E*) also increasing from 1.0 to 1.8 (Table 5, Fig. 6). The yield of cyclohexene oxide follows the trend  $1 > 4 > 5 \approx 2 > 3$ , which is the same as that observed for cyclooctene. This illustrates that the yield of epoxide product is strongly influenced by the electron density on Mn(II) center, as dictated by the linear tetradentate ligand backbone. Upon varying the backbone from L1 to L4 to L5 (or L3) the electron density around the metal center decreases (cf. above), leading to decrease in stability of the high-valent manganese-oxo intermediate and/or discouragement in the in-cage electronic rearrangement, as for the epoxidation of cyclooctene, and hence the decrease in both the yield and selectivity of epoxide product from 1 to 4 to 5 (or 3).

The reaction of styrene with PhIO in the presence of 1–5 has been also investigated under the same reaction conditions described above for cyclooctene and cyclohexene. In addition to major amounts of styrene oxide (17–47%; Table 4, Fig. 7), small amount of benzaldehyde (11–18%) is also obtained as a side product. The yield of styrene oxide follows the trend  $1 > 4 > 2 \approx 5 > 3$ , which is the same as that observed above for cyclooctene and cyclohexene (Scheme 5). This variation is explained based on the variation in stability of the reactive high-valent metal–oxo intermediate



**Scheme 5.** Proposed mechanisms for epoxidation of styrene by using Mn(II) complexes and PhIO epoxide obtained (62–77%) in the presence of *N*-Melm is higher than that obtained in its absence (Table 5, Fig. 8).

and/or to the variation in ease of the in-cage electronic rearrangement in the carbo cation. Such a catalyst–oxidant adduct could deliver the oxygen atom to the substrate and bypass the metal–oxo intermediate if the formation of the metal–oxo species from the oxidant–catalyst adduct is relatively slow compared to the oxygen atom transfer to the substrate (Scheme 5B), which is similar to the mechanism proposed by Collman et al. [52]. The amount of benzaldehyde detected in the  $N_2$  atmosphere is lower than that in the presence of oxygen supporting its formation through further oxidation of the carbo cation directly by oxygen or through C=C cleavage (Scheme 5C) [53,57]. Also, the yield of proposed mechanisms illustrate that for all the olefins the epoxide yield increases upon increasing the electron density on the metal center. The negative charge built on the Mn(II) center facilitates the in-cage electronic rearrangement in the carbo cation and also stabilises the high-valent manganese–oxo intermediate, which has been invoked as the key intermediate responsible for olefin oxidation by both the metalloenzymes [58] and their model complexes [59]. Also, the complexes with less positive Mn(II)/Mn(III) redox potentials are expected to stabilize the high-valent metal–oxo species to a larger extent leading to the formation of higher amount of the epoxide. This reveals that the Lewis acidity of the Mn(II) center, as dictated by the ligand donor environment, plays a vital role in dictating the variation in product yield.

#### 4. Conclusions

The mononuclear Mn(II) complexes of linear tetradentate 4N ligands with sterically demanding diazacycloalkane backbone exhibit varying coordination geometries like distorted octahedral, distorted pentagonal bipyramidal and distorted trigonal prism. In acetonitrile solution they catalyze the epoxidation of *cis*-cyclooctene by using PhIO as the oxygen source to form *cis*-epoxide with high conversion (21–54%) and high selectivity (100%) and the product yield increases (23–64%) upon adding *N*-methylimidazole. Both the product yields and selectivity are higher for the epoxidation of cyclooctene than those for cyclohexene and styrene. The epoxide yield and selectivity decreases upon increasing the Lewis acidity of the Mn(II) center, as modified by diazacycloalkane ligand backbone. The present study reveals that an efficient and robust Mn(II) catalytic system for olefin epoxidation can be designed by having 4N ligands with high Lewis basicity and low steric demand.

#### Acknowledgements

We sincerely thank the Department of Science and Technology, New Delhi, for supporting this research (Scheme No. SR/S5/BC-05/2006), Professor M. Palaniandavar is a recipient of DST Ramanna Fellowship (SR/S1/RFC-01/2010). This work was also supported by Indo-French Centre (IFCPAR) (Scheme No. IFC/A/4109-1/2009/993). UGC-RFMS fellowship to N.S. We thank Department of Science and Technology (FIST Programme) for X-ray diffractometer and UGC-SAP for instrumentation facility at School of Chemistry, Bharathidasan University.

#### Appendix A. Supplementary material

Crystallographic data for **4**, Tables S1, S2 and Fig. S2. CCDC 813736–813739 contain the supplementary crystallographic data for the crystal structures of **1**, **3**, **5** and **4**, respectively. These data can be obtained free of charge from The Cambridge Crystallographic Data Centre via [www.ccdc.cam.ac.uk/data\\_request/cif](http://www.ccdc.cam.ac.uk/data_request/cif). Supplementary data associated with this article can be found, in the online version, at [doi:10.1016/j.ica.2012.01.009](https://doi.org/10.1016/j.ica.2012.01.009).

#### References

- [1] (a) R.A. Johnson, K.B. Sharpless, in: I. Ojima (Ed.), *Catalytic Asymmetric Synthesis*, VCH, New York, 1993, Chapter 4.1.; (b) E.N. Jacobsen, in: I. Ojima (Ed.), *Catalytic Asymmetric Synthesis*, VCH, New York, 1993, Chapter 4.2.
- [2] B. Meunier (Ed.), *Biomimetic Oxidations Catalyzed by Transition Metal Complexes*, Imperial College Press, London, 2000.
- [3] D.N. Vaz, D.F. McGinnity, M.J. Coon, *Proc. Natl. Acad. Sci. U S A* 95 (1998) 3555.
- [4] (a) B.S. Lane, K. Burgess, *Chem. Rev.* 103 (2003) 2457; (b) M. Costas, L. Que, *Chem. Rev.* 104 (2004) 939.
- [5] T.J. Meyer, M.H.V. Huynh, H.H. Thorp, *Angew. Chem.* 119 (2007) 5378.
- [6] (a) D.C. Wealtherburn, S. Mandal, S. Mukhopathyay, S. Bhaduri, L.F. Lindoy, J.A. Cleverty, T.J. Meyer (Eds.), *Comprehensive Coordination Chemistry II*, vol. 4, Elsevier, Pergamon, 2004, p. 1. Chapter 4; (b) A. Sigel, H. Sigel, *Manganese and Its Role in Biological Processes*, Marcel Dekker, New York, 2000.
- [7] D.P. Kessissoglou, *Coord. Chem. Rev.* 185 (1999) 837.
- [8] (a) B. Meunier, *Chem. Rev.* 92 (1992) 1411; (b) T. Katsuki, *Coord. Chem. Rev.* 140 (1995) 189.
- [9] (a) K.A. Jørgensen, *Chem. Rev.* 89 (1989) 431; (b) T. Katsuki, *Adv. Synth. Catal.* 344 (2002) 131; (c) D.E. De Vos, B.F. Sels, P.A. Jacobs, *Adv. Synth. Catal.* 345 (2003) 457.
- [10] Y. Watanabe, A. Namba, N. Umezawa, M. Kawahata, K. Yamaguchi, T. Higuchi, *Chem. Commu.* (2006) 4958.
- [11] W. Zhang, E.N. Jacobsen, *J. Org. Chem.* 56 (1991) 2296.

- [12] W. Zhang, J.L. Loebach, S.R. Wilson, E.N. Jacobsen, *J. Am. Chem. Soc.* 112 (1990) 2801.
- [13] M. Palucki, G.J. McCormick, E.N. Jacobsen, *Tetrahedron Lett.* 36 (1992) 2109.
- [14] D.E. Vos, T. Bein, *J. Organomet. Chem.* 520 (1996) 195.
- [15] (a) E.N. Jacobsen, W. Zhang, A.R. Muci, J.R. Ecker, L. Deng, *J. Am. Chem. Soc.* 113 (1991) 7063;  
(b) J.F. Larrow, E.N. Jacobsen, Y. Gao, Y. Hong, X. Nie, C.M. Zepp, *J. Org. Chem.* 59 (1994) 1939.
- [16] (a) N. Hosoya, ; A. Hatayama, ; K. Yanai, H. Fujii, ; R. Irie, T. Katsuki, *Synlett* (1993) 641;  
(b) R. Irie, K. Noda, Y. Ito, N. Matsumoto, T. Katsuki, *Tetrahedron Lett.* 31 (1990) 734;  
(c) R. Irie, N. Hosoya, T. Katsuki, *Synlett* (1994) 255.
- [17] (a) A. Murphy, G. Dubois, T.D.P. Stack, *J. Am. Chem. Soc.* 125 (2003) 5250;  
(b) A. Murphy, A. Pace, T.D.P. Stack, *Org. Lett.* 6 (2004) 3119;  
(c) A. Murphy, T.D.P. Stack, *J. Mol. Cat. A: Chem.* 251 (2006) 73.
- [18] (a) L. Gomez, I.G. Bosch, A. Company, X. Sala, X. Fontrodona, X. Ribas, M. Costas, *Dalton Trans.* (2007) 5539;  
(b) I.G. Bosch, A. Company, X. Fontrodona, X. Ribas, M. Costas, *Org. Lett.* 10 (2008) 2095.
- [19] D. Pijper, P. Saisaha, J. Joannes W. De Boer, R. Hoen, C. Smit, A. Meetsma, R. Hage, R.P. Van Summeren, P.L. Alsters, B.L. Feringa, W.R. Browne, *Dalton Trans.* 39 (2010) 10375.
- [20] (a) E.G. Samsel, K. Srinivasan, J.K. Kochi, *J. Am. Chem. Soc.* 107 (1985) 7606;  
(b) K. Srinivasan, P. Michaud, J.K. Kochi, *J. Am. Chem. Soc.* 108 (1986) 2309.
- [21] (a) C.L. Hill, B.C. Schardt, *J. Am. Chem. Soc.* 102 (1980) 6374;  
(b) J.T. Groves, W. Kruper, R.C. Haushalter, *J. Am. Chem. Soc.* 102 (1980) 6375.
- [22] K. Nehru, S.J. Kim, I.Y. Kim, M.S. Seo, Y. Kim, S.J. Kim, J. Kim, W. Nam, *Chem. Commun.* (2007) 4623.
- [23] (a) P. Battioni, J.P. Renaud, J.F. Bartoli, M. Reina-Arilles, M. Fort, D. Mansuy, *J. Am. Chem. Soc.* 110 (1988) 8462;  
(b) Feichtinger, D.A. Plattner, *Angew. Chem., Int. Ed. Engl.* 36 (1997) 5457;  
(c) T.J. Collins, R.D. Powell, C. Siebodnick, E.S. Uffelman, *J. Am. Chem. Soc.* 112 (1990) 899;  
(d) T.J. Collins, S.W. Gordon-Wyllie, *J. Am. Chem. Soc.* 111 (1989) 4511.
- [24] (a) F.M. Macdonnell, N.L.P. Fackler, C. Stern, T.V. O'Halloran, *J. Am. Chem. Soc.* 116 (1994) 7431;  
(b) N.S. Finney, P.J. Pospisil, S. Chang, M. Palucki, R.G. Konsler, K.B. Hansen, E.N. Jacobsen, *Angew. Chem., Int. Ed. Engl.* 36 (1997) 1720;  
(c) B. Meunier, E. Guilmet, M. De arvalho, R. Poilblanc, *J. Am. Chem. Soc.* 122 (2000) 2675.
- [25] (a) J.T. Groves, J. Lee, S.S. Marla, *J. Am. Chem. Soc.* 119 (1997) 6269;  
(b) N. Jin, J.T. Groves, *J. Am. Chem. Soc.* 121 (1999) 2923;  
(c) N. Jin, J.L. Bourassa, S.C. Tizio, J.T. Groves, *Angew. Chem.* 112 (2000) 4007;  
(d) N. Jin, J.L. Bourassa, S.C. Tizio, J.T. Groves, *Angew. Chem., Int. Ed.* 39 (2000) 3849;  
(e) F. De Angelis, N. Jin, R. Car, J.T. Groves, *Inorg. Chem.* 45 (2006) 4268.
- [26] (a) W. Nam, I. Kim, M.H. Lim, H.J. Choi, J.S. Lee, H.G. Jang, *Chem. Eur. J.* 8 (2002) 2067;  
(b) W.J. Song, M.S. Seo, S.D. George, T. Ohta, R. Song, M.-J. Kang, T. Tosha, T. Kitagawa, E.I. Solomon, W. Nam, *J. Am. Chem. Soc.* 129 (2007) 1268;  
(c) J.Y. Lee, Y.-M. Lee, H. Kotani, W. Nam, S. Fukuzumi, *Chem. Commun.* (2009) 704;  
(d) C. Arunkumar, Y.-M. Lee, J.Y. Lee, S. Fukuzumi, W. Nam, *Chem. Eur. J.* 15 (2009) 11482;  
(e) S. Fukuzumi, N. Fujioka, H. Kotani, K. Ohkubo, Y.-M. Lee, W. Nam, *J. Am. Chem. Soc.* 131 (2009) 17127.
- [27] (a) R. Zhang, M. Newcomb, *J. Am. Chem. Soc.* 125 (2003) 12418;  
(b) R. Zhang, J.H. Horner, M. Newcomb, *J. Am. Chem. Soc.* 127 (2005) 6573.
- [28] (a) Y. Shimazaki, T. Nagano, H. Takesue, B.-H. Ye, F. Tani, Y. Naruta, *Angew. Chem., Int. Ed.* 116 (2004) 100;  
(b) Y. Shimazaki, T. Nagano, H. Takesue, B.-H. Ye, F. Tani, Y. Naruta, *Angew. Chem., Int. Ed.* 43 (2004) 98.
- [29] (a) G. Yin, A.M. Danby, D. Kitko, J.D. Carter, W.M. Scheper, D.H. Busch, *J. Am. Chem. Soc.* 129 (2007) 1512;  
(b) G. Yin, A.M. Danby, D. Kitko, J.D. Carter, W.M. Scheper, D.H. Busch, *J. Am. Chem. Soc.* 130 (2008) 16245;  
(c) T. Kurahashi, A. Kikuchi, T. Tosha, Y. Shiro, T. Kitagawa, H. Fujii, *Inorg. Chem.* 47 (2008) 1674;  
(d) T. Kurahashi, A. Kikuchi, Y. Shiro, M. Hada, H. Fujii, *Inorg. Chem.* 49 (2010) 6664.
- [30] (a) T.H. Parsell, R.K. Behan, M.T. Green, M.P. Hendrich, A.S. Borovik, *J. Am. Chem. Soc.* 128 (2006) 8728;  
(b) T.H. Parsell, M.Y. Yang, A.S. Borovik, *J. Am. Chem. Soc.* 131 (2009) 2762;  
(c) R.L. Shook, A.S. Borovik, *Inorg. Chem.* 49 (2010) 3646;  
(d) S.C. Savant, X. Wu, J. Cho, K.B. Cho, S.H. Kim, M.S. Seo, Y.M. Lee, M. Kubo, T. Ogura, S. Shaik, W. Nam, *Angew. Chem., Int. Ed.* 49 (2010) 8190.
- [31] T. Kurahashi, A. Kikuchi, T. Tosha, Y. Shiro, T. Kitagawa, H. Fujii, *Inorg. Chem.* 4 (2008) 1674.
- [32] Z. Li, C.G. Xia, M. Ji, *Appl. Catal. A: General* 252 (2003) 17.
- [33] C. Hureau, G. Blondin, M.F. Charlot, C. Philauze, M. Neirlich, M. Césario, E. Anxolabéhère-Mallart, *Inorg. Chem.* 44 (2005) 3669.
- [34] C. Baffert, M. Collomb, A. Deronzier, S. Kjaegaard-Knudsen, J. Latour, K. Lund, C. McKenzie, L. Martin Mortensen, Nielsen, T. Niels, *Dalton Trans.* (2003) 1765.
- [35] J.A. Halfen, J.M. Uhan, D.C. Fox, M.P. Mehn, L. Que Jr., *Inorg. Chem.* 39 (2000) 4913.
- [36] R. Mayilmurugan, H. Stoeckli Evans, M. Palaniandavar, *Inorg. Chem.* 47 (2008) 6645.
- [37] G.M. Sheldrick, SAINT 5.1, Siemens Industrial Automation Inc., Madison, WI, 1995.
- [38] SADABS, Empirical Absorption Correction Program, University of Göttingen, Göttingen, Germany, 1997.
- [39] G.M. Sheldrick, SHELXTL Reference Manual: Version 5.1, Bruker AXS, Madison, WI, 1997.
- [40] G.M. Sheldrick, SHELXS-97: Program for the Solution of Crystal Structure, University of Göttingen, Göttingen, Germany.
- [41] G.S. Girolami, T.B. Rauchfuss, R.J. Angelici, *Synthesis and Technique in Inorganic Chemistry*, third ed., University Science Books, Sausalito, 1999.
- [42] (a) K.R.J. Thomas, M. Velusamy, M. Palaniandavar, *Acta Crystallogr., Sect. C* 54 (1998) 741;  
(b) D. Mandon, A. Nopper, T. Litrol, S. Goetz, *Inorg. Chem.* 40 (2001) 4803;  
(c) M.C. Rodriguez, F. Lambert, I. Morgenstern-Badarau, M. Cesario, J. Guilhem, B. Keita, L. Nadjio, *Inorg. Chem.* 36 (1997) 3525;  
(d) D. Stefen, W. Armin, W. Ursel, W. Friedrich, G.Z. Gerhard, *Naturforsch. B: Chem. Sci.* 52 (1997) 372;  
(e) M. Velusamy, R. Mayilmurugan, M. Palaniandavar, *J. Inorg. Biochem.* 99 (2005) 1032.
- [43] (a) A.R. Geiger, A.S. Chattopadhyay, W.V. Day, A.T. Jackson, *J. Am. Chem. Soc.* 132 (2010) 2821;  
(b) A.R. Geiger, A.S. Chattopadhyay, W.V. Day, A.T. Jackson, *Dalton Trans.* 40 (2011) 1707.
- [44] K. Chen, L. Que, *Angew. Chem., Int. Ed.* 38 (1999) 2227.
- [45] J.E. Huheey, E.A. Keiter, R.L. Keiter, O.K. Medhi, *Inorganic Chemistry*, Pearson Ed. Inc., USA, 1993, Chapter 14.
- [46] A. Halfen, L. Moore, C. Fox, *Inorg. Chem.* 41 (2002) 3935.
- [47] B. Manindranath, B. Kumar, Debahis Ray, *Inorg. Chimica. Acta.* 357 (2004) 3556.
- [48] (a) K. Visvaganesan, R. Mayilmurugan, E. Suresh, M. Palaniandavar, *Inorg. Chem.* 46 (2007) 10294;  
(b) K. Sundaravel, T. Dhanalakshmi, E. Suresh, M. Palaniandavar, *Dalton Trans.* (2008) 7012.
- [49] M. Sono, M.P. Roach, E.D. Coulter, J.H. Dawson, *Chem. Rev.* 96 (1996) 2841.
- [50] T. Yamada, K. Imagawa, K. Nagata, T. Mukaiyama, *Chem. Lett.* (1992) 2231.
- [51] P. Pietikäinen, *Tetrahedron Lett.* 35 (1994) 941;  
(b) P. Battioni, J.P. Renaud, J.F. Bartoli, M. Reina-Arilles, M. Fort, D. Mansuy, *J. Am. Chem. Soc.* 110 (1988) 8462.
- [52] (a) J.P. Collman, A.S. Chien, T.A. Eberspacher, J.I. Brauman, *J. Am. Chem. Soc.* 122 (2000) 11098;  
(b) J.P. Collman, L. Zeng, R.A. Decreau, *Chem. Commun.* (2003) 2974;  
(c) J.P. Collman, L. Zeng, J.I. Brauman, *Inorg. Chem.* 43 (2004) 2672.
- [53] M. Murali, R. Mayilmurugan, M. Palaniandavar, *Eur. J. Inorg. Chem.* 22 (2009) 3238.
- [54] (a) K. Jitsukawa, Y. Oka, S. Yamaguchi, H. Masuda, *Inorg. Chem.* 43 (2004) 8119;  
(b) L.K. Stultz, M.H.V. Huynh, R.A. Binstead, M. Curry, T.J. Meyer, *J. Am. Chem. Soc.* 122 (2000) 5984.
- [55] A.J. Appleton, S. Evans, J.R. Lindsay Smith, *J. Chem. Soc., Perkin Trans. 2* (1996) 281.
- [56] (a) F.R. Mayo, *Acc. Chem. Res.* 1 (1968) 193;  
(b) D.R. Paulson, R. Ullman, R.B. Sloan, *J. Chem. Soc., Chem. Commun.* (1974) 186.
- [57] (a) W.-H. Fung, W.-Y. Yu, C.-M. Che, *J. Org. Chem.* 63 (1998) 7715;  
(b) C.-J. Liu, W.-Y. Yu, C.-M. Che, C.-H. Yeung, *J. Org. Chem.* 64 (1999) 7365.
- [58] (a) C. Mantel, A. Hassan, J. Pecaut, A. Deronzier, M.N. Collomb, C. Duboc-Toia, *J. Am. Chem. Soc.* 125 (2003) 12337;  
(b) W. Adam, K.J. Roschmann, C.R.Saha-Möller, D. Seebach, *J. Am. Chem. Soc.* 124 (2002) 5068.
- [59] (a) M. Palucki, N.S. Finney, P.J. Pospisil, Guler, M.L.T. Ishida, E.N. Jacobsen, *J. Am. Chem. Soc.* 120 (1998) 948;  
(b) T. Linker, *Angew. Chem., Int. Ed.* 36 (1997) 2060.